

Multi-User Detection in Multicarrier-CDMA Systems

Dr.-Ing. Volker Kühn

Ronald Böhnke

Prof. Dr.-Ing. Karl-Dirk Kammeyer

Universität Bremen,

Department of Communications Engineering

Kufsteiner Straße NW 1

D-28359 Bremen, Germany

{kuehn, boehnke, kammeyer}@ant.uni-bremen.de

Manuscript for e&i-Journal

Abstract:

The upcoming third generation mobile radio system in Europe is based on UMTS (Universal Mobile Telecommunications Standard). In order to supply access to a common transmission channel for several users, UMTS incorporates Code Division Multiple Access (CDMA). Besides a lot of practical advantages, CDMA suffers from multi-user interference limiting spectral efficiency dramatically. However, bandwidth is a very valuable resource and should be used as efficiently as possible. One appropriate mean to increase spectral efficiency of CDMA systems is multi-user detection.

This paper gives an overview of different multi-user detection techniques. Their performance is compared with the conventional single-user detection including channel coding. Specifically, linear as well as nonlinear multi-user detectors are considered. Efficient realizations of linear detectors are given leading to improved nonlinear techniques. It is shown that nonlinear MUD including channel decoding can achieve a spectral efficiency twice as high as that of the well-known GSM standard (Global System for Mobile Communications) employing TDMA and FDMA.

I. Introduction

Mobile radio communication has become a rapidly growing market since the GSM standard [1] has been established. Meanwhile, third generation mobile radio systems like UMTS and CDMA 2000 have been standardized [2,3,4] and the fourth generation is currently under investigation. During this development, Code Division Multiple Access has become a widely accepted multiple access technique. In most cases, it is implemented as Direct-Sequence CDMA (DS-CDMA) in single-carrier (SC) systems.

Alternatively, multi-carrier CDMA (MC-CDMA) offers a lot of advantages over single-carrier systems [5,6,7,8]. Here, the entire bandwidth is divided into narrow sub-channels. When OFDM (Orthogonal Frequency Division Multiplexing) is employed, these sub-channels are orthogonal and do not mutually interfere. A single chip now occupies only a small fraction of the whole bandwidth. Therefore, it is affected by flat fading and a one-tap-equalizer suffices for eliminating channel distortion.

In this paper, we mainly consider the uplink of an OFDM-CDMA transmission. Due to frequency selective fading and asynchronously transmitting subscribers, the orthogonality of scrambling codes cannot be maintained. Hence, pseudo-random sequences are employed causing severe multi-user interference (MUI) that degrades the system performance and limits system capacity. Two possibilities for combating this degradation are discussed.

First, the interference is treated as white gaussian noise and the overall system performance is improved by strong error control coding that shows a good performance especially at low signal-to-noise ratios. Due to the inherent spreading in CDMA systems, each user occupies a very large bandwidth and low rate channel coding with potentially high coding gains can be employed. In [9] it is shown that strong low rate error control codes, e.g. a serial concatenation of interleaved convolutional and Walsh-Hadamard codes, are able to ensure a reliable transmission for low and medium system loads.

Second, multi-user detection (MUD) techniques can be applied to eliminate MUI [10,11,12]. These methods exploit the deterministic structure of the interference but require higher computational costs especially for asynchronous transmission. The application of OFDM reduces these costs because each chip is only affected by flat fading. For high loads, i.e. the number of active users reaches or even exceeds the CDMA spreading factor, multi-user detection is necessary to combat MUI efficiently. Here, linear and nonlinear schemes as well as a combination of both can be applied [13,14].

This paper has the following structure: After this introduction, the fundamentals of OFDM-CDMA are described. Based on this description, the performance of a single-user detector is analyzed taking channel coding into account. Section IV then presents an overview of multi-user detection schemes, incorporating linear and nonlinear approaches. The performance of different techniques is demonstrated by simulation results. Finally, some conclusions summarize the paper.

II. Fundamentals of OFDM-CDMA

The analysis in this paper is based on an OFDM-CDMA system whose structure is depicted in Figure 1. The bits $d_u(i)$ at time instance i for each user $u = 1 \dots U$ are of duration T_d . They are spread by repeating each bit N_s times and successive multiplication with a user-specific code $\mathbf{c}_u(i)$ (Direct-Sequence CDMA). Throughout the paper, the duration of one chip $c_u(i, k)$ equals $T_c = T_d / N_s$ where k represents the time instance for a certain chip¹. For a synchronous downlink, orthogonal spreading codes can be employed to keep the level of interference as low as possible. For an asynchronous uplink transmission, orthogonality cannot be maintained and simple pseudo-noise (PN) sequences are used for spreading.

Next, the OFDM transmitter transforms the obtained vector into the time domain. According to Figure 1, it consists of a serial-parallel converter that maps N_c chips onto different subcarriers. After subsequent interleaving in frequency domain (Π_f), an inverse Fourier transformation (IFFT) and a parallel-serial conversion are performed. Finally, a cyclic prefix called guard interval of duration T_g is inserted in front of each OFDM symbol. A guard time T_g larger than the delay-spread $\Delta\tau$ of the channel ensures a cyclic convolution of $x_u(l)$ with the channel impulse response $h_u(i, l)$ resulting in an element-wise multiplication in frequency domain. Hence, each chip is only affected by flat fading. With the channel transfer function

$$H_u(i, k) = \sum_{l=0}^{L-1} h_u(i, l) \cdot e^{-j2\pi kl/L}, \quad (1)$$

¹ Usually, $c_u(i, k) = 0$ holds for $k < iN_s$ and $k \geq (i+1)N_s$, i.e. there is no overlapping between spreading codes of successive bits. For so-called short codes, $c_u(i, k)$ is periodic in i .

the so-called signature is defined by

$$s_u(i, k) = H_u(i, k) \cdot c_u(i, k). \quad (2)$$

In (1), real and imaginary parts of the channel coefficients $h_u(i, l)$ are gaussian distributed and statistically independent. Although each user is assigned to an individual channel, the number of transmission paths L is assumed to be the same for all users.

The received signal $\tilde{y}(l)$ consists of the desired signal $x_u(l)$, the interfering signals of other users (MUI) and the background noise $n(l)$. For the downlink, all interfering signals are affected by the same channel, whereas in the uplink, each user is transmitting over an individual mobile radio channel.

Throughout this work, a coarse synchronization is assumed, i.e. the maximum delay between different users is limited to $T_g - \Delta\tau$. In this case, one FFT window suffices for all users and the OFDM-CDMA receiver has a structure depicted in Figure 2. It consists of a common OFDM part and a user-specific CDMA part described in the next section. In the OFDM receiver, the cyclic prefix is removed first. Due to the cyclic convolution of $x_u(l)$ and $h_u(i, l)$ the transformation back into the frequency domain can be efficiently realized by the fast Fourier transform (FFT). After de-interleaving and parallel-serial conversion, the obtained signal can be mathematically expressed by

$$y(k) = \sum_i \sum_{u=1}^U d_u(i) \cdot s_u(i, k) + n(k). \quad (3)$$

A more convenient description can be obtained by using vector notations. Comprising all samples $y(k)$ with $iN_s \leq k < (i+1)N_s$ to a vector $\mathbf{y}(i)$ and neglecting the time index i , yields

$$\mathbf{y} = \mathbf{S} \cdot \mathbf{d} + \mathbf{n}, \quad (4)$$

where the u -th column of \mathbf{S} is defined by $\mathbf{s}_u = [s_u(0) \cdots s_u(N_s - 1)]^T$ and $\mathbf{d} = [d_1 \cdots d_U]^T$ holds².

The next section analyzes the optimal single-user detector.

² Due to the insertion of the guard interval, successive OFDM symbols are treated separately and the time index i can be neglected for simplicity.

III. Single-User Detection

The optimal single-user detector treats multi-user interference as white gaussian noise and consists of a bank of user-specific matched filters. For DS-CDMA, matched filtering is performed by correlating $y(k)$ with the conjugate complex signature sequence $s_u^*(i, k)$. Using again the vector notation, the outputs of all matched filters are comprised to a vector

$$\mathbf{r} = \mathbf{S}^H \cdot \mathbf{y} = \mathbf{S}^H \mathbf{S} \cdot \mathbf{d} + \mathbf{S}^H \cdot \mathbf{n} \quad (5)$$

If the signatures in \mathbf{S} are orthogonal, the correlation matrix $\mathbf{S}^H \mathbf{S}$ in (5) is diagonal. Under these conditions, no multi-user interference is present and the single-user matched filter would be optimal. However, in most practical cases \mathbf{S} is not unitary, $\mathbf{S}^H \mathbf{S}$ is not diagonal and MUI severely limits the system performance. For BPSK modulation, only the real part of \mathbf{r} is important. Thus, the estimates of the transmitted bits are obtained by $\hat{\mathbf{d}} = \text{Re}\{\mathbf{r}\}$.

Analyzing (5) for user 1 yields the expression

$$r_1 = \sum_{k=0}^{N_s-1} s_1^*(k) \cdot \sum_{u=1}^U d_u \cdot s_u(k) + n(k) = d_1 \cdot \Phi_{1,1} + \sum_{u=2}^U d_u \cdot \Phi_{1,u} + \eta \quad (6)$$

Obviously, r_1 consists of the desired symbol d_1 weighted with the autocorrelation coefficient $\Phi_{1,1}$ of signature s_1 , the multi-user interference influenced by the crosscorrelation coefficients $\Phi_{1,u}$ between s_1 and all other s_u and a noise term η .

As already mentioned, this matched filter treats the interference in (6) as white gaussian noise. In this case, it is known from information theory [12] that the best thing to do is the application of powerful low rate coding at the expense of smaller spreading factors. Therefore, the bits d_u represent the output of a channel encoder and the signal \hat{d}_u in Figure 2 must be finally fed to an appropriate channel decoder.

In [9,15], it was shown that CDMA spreading can be interpreted as a simple repetition code with successive scrambling. Therefore, the inherent spreading in CDMA systems can be used for applying very low rate coding without further bandwidth expansion, e.g. the poor repetition code can be replaced by a strong serially concatenated code [9]. Such a code has to be iteratively decoded according to the “turbo-principle” [16]. For a chip-synchronous transmission and

random spreading codes, the resulting signal-to-interference-plus-noise-ratio at the decoder inputs has the form

$$SINR = \frac{N_s \cdot E_c / N_0}{1 + (U - 1) \cdot E_c / N_0} = \frac{R_c \cdot E_b / N_0}{1 + (U - 1) / N_s \cdot R_c \cdot E_b / N_0}. \quad (7)$$

In (7), E_c and E_b denote the energies per chip and per information bit, respectively, whereas R_c represents the code rate of the applied channel code. In the sequel, $\beta = U / N_s$ denotes the load of a system.

Figure 3 depicts the bit error rate performance of an uncoded OFDM-CDMA system employing a conventional convolutional code for different number of active users. Obviously, the performance degrades dramatically for increasing β . Therefore, spectral efficiency of CDMA with single-user detection is strictly interference limited.

However, strong error control coding can achieve acceptable error rates for low and medium loads. The performance of different coding scenarios for an OFDM-CDMA system is shown in Figure 4. Here, the concatenated coding scheme achieves error rates of 10^{-6} and below. However, the required E_b / N_0 is increased and, therefore, power efficiency is reduced. The codes discussed in [9] represent just some examples to demonstrate that strong error control is able to combat MUI for appropriate system loads. They are not optimal in the sense that channel capacity is reached. For higher loads $\beta > 1$, solely coding may become very difficult and even costly in terms of computational costs. Therefore, it is advisable to apply multi-user detection as described in the following section.

IV. Multi-User Detection

As mentioned in the previous section, the conventional single-user detector treats MUI as white gaussian noise. However, the interference caused by simultaneously transmitting users in a CDMA-system is actually highly structured and can be modeled by a (possibly time-varying) cyclostationary process [11]. This fact can be exploited resulting in considerable performance gains. We will mainly focus on the case where all signature sequences are known at the receiver site, i.e. the base station for uplink transmission. Nevertheless, section IV.3. illuminates one of the main advantages of OFDM-CDMA over single-carrier variants, namely the strong relation between linear MUD in the downlink and simple equalization of the received signal with the aim of restoring the orthogonality between users. Therefore, just like for much more sophisticated so-

called blind algorithms (see e.g. [11,18]), no knowledge of the interfering users' signatures is required.

First of all, the optimal detector is introduced together with some slight modifications. The corresponding decision regions are illustrated by a simple two-user example. Afterwards, linear MUD is treated in detail. Particular attention is spent on efficient iterative algorithms to approximate the solution of the underlying linear equation systems. Further significant improvements arise from the combination of such iterative interference cancellation schemes with nonlinear components and channel decoding to mitigate the effect of error propagation.

IV.1. Optimal MUD

In order to minimize the number of erroneous decisions, the receiver needs to choose the symbol \hat{d}_u transmitted most likely by the user u , based on the observation of the received signal \mathbf{y} . Thus, optimal MUD follows from utilizing the maximum-a-posteriori criterion (MAP)

$$\hat{d}_u = \arg \max_{d_u \in \{-1,1\}} P(d_u | \mathbf{y}) \quad (8)$$

for each user individually. By applying Bayes' rule $P(d_u | \mathbf{y}) = p(\mathbf{y} | d_u) \cdot P(d_u) / p(\mathbf{y})$ and ignoring the term $p(\mathbf{y})$ which is independent of the hypothesis d_u , we arrive at a more convenient MAP-formulation

$$\hat{d}_u = \arg \max_{d_u \in \{-1,1\}} p(\mathbf{y} | d_u) \cdot P(d_u). \quad (9)$$

Note that $p(\mathbf{y} | d_u) \cdot P(d_u)$ can be expressed as the sum over all $p(\mathbf{y} | \mathbf{d}) \cdot P(\mathbf{d})$ with d_u kept fixed in \mathbf{d} . In presence of white gaussian noise, $p(\mathbf{y} | \mathbf{d}) \propto \exp(-\|\mathbf{y} - \mathbf{S}\mathbf{d}\|^2 / \mathbf{s}_n^2)$ holds which rapidly degenerates into a narrow pulse for small noise power. In this case, all sums over $p(\mathbf{y} | \mathbf{d}) \cdot P(\mathbf{d})$ for different fixed d_u are dominated by the same term with maximum $p(\mathbf{y} | \mathbf{d})$ leading to the joint-maximum-a-posteriori criterion (JMAP)

$$\hat{\mathbf{d}} = \arg \max_{\mathbf{d} \in \{-1,1\}^U} p(\mathbf{y} | \mathbf{d}) \cdot P(\mathbf{d}). \quad (10)$$

If transmit symbols are assumed to be independent and equiprobable the a-priori probabilities in (9) and (10) do not influence the maximization and can be neglected. The so modified decision

rules are called maximum-likelihood (ML) and joint-maximum-likelihood (JML), respectively. With $p(\mathbf{y}|\mathbf{d})$ as given above, the JML criterion is equivalent to

$$\hat{\mathbf{d}} = \arg \min_{\mathbf{d} \in \{-1,1\}^U} \|\mathbf{y} - \mathbf{S}\mathbf{d}\|^2, \quad (11)$$

i.e. $\hat{\mathbf{d}}$ is chosen to minimize the distance between the actual receive vector \mathbf{y} and the noiseless estimate $\mathbf{S}\hat{\mathbf{d}}$.

The optimal decision borders for user 1 are demonstrated in Figure 5a by means of a simple two-user example with signatures $\mathbf{s}_1 = [1,0]^T$ and $\mathbf{s}_2 = [0.6,0.8]^T$ and equiprobable transmit symbols. For low noise level ($E_b/N_0 = 20\text{dB}$), joint detection by minimum distance decision is optimal while in the opposite limit the matched filter proves to be best because MUI is negligible in that case. In general, the MAP boundaries are smoothed versions of the JML ones.

Under certain circumstances optimal MUD can be treated with polynomial complexity [10,19]. However, the problem is NP-complete in general, i.e. the computational effort grows exponentially with the number of active users. Hence, it is not practicable for high system loads, and suboptimal but less demanding alternatives to mitigate the effect of MUI have to be used.

IV.2. Linear MUD

Linear multi-user receivers have been extensively studied during the past decade [10,20]. Here, a linear transformation is applied to the received signal in order to remove or at least reduce MUI. Recalling the output of the matched filter $\mathbf{r} = \mathbf{S}^H \mathbf{y} = \mathbf{S}^H \mathbf{S} \mathbf{d} + \mathbf{S}^H \mathbf{n}$, a straightforward approach would be to invert the square matrix $\mathbf{S}^H \mathbf{S}$

$$\hat{\mathbf{d}} = (\mathbf{S}^H \mathbf{S})^{-1} \mathbf{S}^H \mathbf{y} = \mathbf{d} + (\mathbf{S}^H \mathbf{S})^{-1} \mathbf{S}^H \mathbf{n} \quad (12)$$

resulting in complete elimination of MUI. Thus, this receiver is called zero-forcing detector or decorrelator. Note that the matrix inverse in (12) does not exist for linearly dependent columns in \mathbf{S} and hence for overloaded systems. In this case, the linear filter $(\mathbf{S}^H \mathbf{S})^{-1} \mathbf{S}^H$ has to be replaced by $\mathbf{S}^H (\mathbf{S} \mathbf{S}^H)^{-1}$ or, more generally, the Moore-Penrose pseudo-inverse \mathbf{S}^+ [21].

It can be shown that the decorrelator minimizes the euclidean distance between \mathbf{y} and $\mathbf{S}\hat{\mathbf{d}}$. Therefore it coincides with the JML detector if \mathbf{d} is not restricted to some discrete alphabet but

can be arbitrarily chosen from the whole U dimensional space \mathbb{R}^U . Nevertheless, the decorrelator behaves poorly for system loads close to one as suppression of MUI is accompanied by a dramatic increase of noise power under these circumstances [22]. A better strategy is to find the linear mapping that maximizes the SINR instead. Interestingly, this is equivalent to minimizing the mean squared error (MSE) between the actually transmitted symbols \mathbf{d} and the estimates $\hat{\mathbf{d}}$ [10]. The solution to this problem is known as MMSE detector and differs from the decorrelator (12) only by adding the noise power to the main diagonal of the matrix to be inverted

$$\hat{\mathbf{d}} = (\mathbf{S}^H \mathbf{S} + \mathbf{s}_n^2 \mathbf{I})^{-1} \mathbf{S}^H \mathbf{y}. \quad (13)$$

When using BPSK modulation one can take advantage of the fact that the data symbols are real. As a consequence, the whole useful signal energy is contained in the real part of the matched filter signal \mathbf{r} while the imaginary part is solely interference and noise and should be suppressed before performing the linear MUD. Furthermore, taking into account that the effective noise power after eliminating the imaginary component is only $\mathbf{s}_n^2 / 2$, we get the MMSE detector tuned to BPSK

$$\hat{\mathbf{d}} = \left(\text{Re}\{\mathbf{S}^H \mathbf{S}\} + \frac{\mathbf{s}_n^2}{2} \mathbf{I} \right)^{-1} \cdot \text{Re}\{\mathbf{S}^H \mathbf{y}\}. \quad (14)$$

Again, the decorrelator for BPSK follows from (14) by setting $\mathbf{s}_n^2 = 0$ [22]. Note that the modified detectors require less computational effort as complex operations are replaced by real ones. Even more important, neglecting the imaginary part of the crosscorrelation matrix $\mathbf{S}^H \mathbf{S}$ has the same effect as halving the number of users leading to a significantly enhanced bit error rate especially for high system loads.

Figure 5b shows the decision regions of the MMSE detector for varying E_b / N_0 . For vanishing noise, the border is parallel to the signature \mathbf{s}_2 resulting in perfect suppression of MUI as for the decorrelator. With increasing noise power, the MMSE detector gradually turns towards the matched filter.

The achievable bit error rates of an MMSE detector according to (14) for BPSK modulation are illustrated in Figure 6. The results have been obtained for an uncoded OFDM-CDMA system with a 4-path Rayleigh fading channel. Compared to the single-user detector in Figure 3, the

improved performance becomes obvious. However, the MMSE detector is not able to totally remove interference and performance degrades for increasing load.

IV.3. Linear MUD for OFDM-CDMA Downlink

Considering downlink transmission, the channel impulse response is the same for all users. Thus, the signature matrix can be written as $\mathbf{S} = \mathbf{H}\mathbf{C}$, where \mathbf{H} is a diagonal matrix containing the channel coefficients in frequency domain and the columns of \mathbf{C} are made up of orthogonal spreading sequences (e.g. Walsh-codes). If the system is not overloaded (i.e. $U \leq N_s$) we can always assume \mathbf{C} to be square, as we can introduce virtual users transmitting zeros without altering the received signal. Then, recalling that $\mathbf{C}^{-1} = \mathbf{C}^H$ for orthogonal sequences, the decorrelator can be written as

$$\hat{\mathbf{d}} = (\mathbf{S}^H \mathbf{S})^{-1} \mathbf{S}^H \mathbf{y} = \mathbf{C}^H (\mathbf{H}^H \mathbf{H})^{-1} \mathbf{H}^H \mathbf{y} = \mathbf{C}^H \mathbf{H}^{-1} \mathbf{y}, \quad (15)$$

allowing an extremely easy realization of MUD by simple linear equalization of the channel and subsequent correlation with the spreading sequences. This procedure is called orthogonal restoring combining (ORC) [8]. Note that just like in far more sophisticated blind algorithms, no knowledge of the interfering users' signatures is required. Equivalently, we can derive a MMSE detector for the OFDM-CDMA downlink

$$\hat{\mathbf{d}} = (\mathbf{S}^H \mathbf{S} + \mathbf{s}_n^2 \mathbf{I})^{-1} \mathbf{S}^H \mathbf{y} = \mathbf{C}^H (\mathbf{H}^H \mathbf{H} + \mathbf{s}_n^2 \mathbf{I})^{-1} \mathbf{H}^H \mathbf{y}. \quad (16)$$

Remember that (15) and (16) will only coincide with the decorrelator and the MMSE-detector, respectively, if the original spreading matrix \mathbf{C} is square, i.e. the system is fully loaded. Otherwise, the additional degrees of freedom introduced by the virtual users will lead to modified results in presence of noise.

IV.4. Iterative Approximations of linear MUD

Though the complexity of linear MUD is much smaller than that of optimal MUD, we still need to invert a matrix of size $U \times U$ involving $O\{U^3\}$ multiplications, in general. In other words, we have to solve a linear equation system $\mathbf{M}\hat{\mathbf{d}} = \mathbf{r}$, where \mathbf{r} is the output of the matched filter and \mathbf{M} determines the type of the detector. However, it often suffices to approximate the solution through iterative algorithms that require only $O\{U^2\}$ operations per iteration.

Solving every single line of the equation system for the \hat{d}_u belonging to the main diagonal element m_{uu} of \mathbf{M} and introducing an iteration index p we get the Jacobi iteration

$$\hat{d}_u^{(p+1)} = \left(r_u - \sum_{v=1}^{u-1} m_{uv} \hat{d}_v^{(p)} - \sum_{v=u+1}^U m_{uv} \hat{d}_v^{(p)} \right) / m_{uu}, \quad (17)$$

i.e. the updated data estimate $\hat{d}_u^{(p+1)}$ for user u is gained from the other users' estimates of the previous step. In context of MUD this procedure is frequently denoted (linear) parallel interference cancellation (PIC) as m_{uv} describes the crosscorrelation between users u and v and, hence, $m_{uv} \hat{d}_v^{(p)}$ is the estimated interference. Unfortunately, this iteration method only converges for low system loads. More precisely, it can be shown for large systems (i.e. $U = \mathbf{b} N_s \rightarrow \infty$) with random spreading that the decorrelator converges for $\mathbf{b} < (\sqrt{2} - 1)^2 \approx 0.17$. A necessary condition for convergence to the MMSE solution is given by $\mathbf{b} < (\sqrt{2 + \mathbf{s}_n^2} - 1)^2$ [23]. Utilizing the BPSK-specific modifications of the receivers that reduce the effective system load and noise power by a factor 2 (cf. section IV.2), the Jacobi algorithm is theoretically applicable for system loads up to $2 \cdot (\sqrt{2 + \mathbf{s}_n^2 / 2} - 1)^2$ which is still quite dissatisfying.

These convergence problems can be overcome if already updated estimates are used immediately when they become available. The corresponding iteration rule reads

$$\hat{d}_u^{(p+1)} = \left(r_u - \sum_{v=1}^{u-1} m_{uv} \hat{d}_v^{(p+1)} - \sum_{v=u+1}^U m_{uv} \hat{d}_v^{(p)} \right) / m_{uu} \quad (18)$$

and is known as Gauss-Seidel algorithm. It can be interpreted as a mixture of parallel and successive interference cancellation (SIC). Observe that now the order of updating (that can easily be changed by permuting rows and columns of \mathbf{M} and the corresponding elements of $\hat{\mathbf{d}}$ and \mathbf{r} , respectively) is crucial whereas Jacobi's method allows a fully parallel implementation.

The excellent performance of Gauss-Seidel iterations is shown in Figure 7. For error rates above 10^{-3} , only minor differences can be observed compared to the MMSE detector. For lower error rates, the curves flatten out. However, it has to be emphasized that error rates above 10^{-3} represent the important region in the uncoded case because subsequent channel coding then leads to an acceptable overall performance. Therefore, the loss of Gauss-Seidel iterations is rather small.

There are various other iterative algorithms for the solution of linear systems known in literature that show superior convergence behaviour, e.g. the conjugate gradient method [21]. It is based on the fact that solving $\mathbf{M}\hat{\mathbf{d}}=\mathbf{r}$ and minimizing the quadratic function $f(\hat{\mathbf{d}})=\hat{\mathbf{d}}^H\mathbf{M}\hat{\mathbf{d}}-2\cdot\text{Re}\{\hat{\mathbf{d}}^H\mathbf{r}\}$ are equivalent goals. The multivariate problem is then broken up into a sequence of one-dimensional minimizations with appropriately chosen linear independent search directions. Another relatively new approach especially suited for OFDM-CDMA is to approximate the MMSE detector by a matrix polynomial [22]. Making use of the Horner scheme we can write

$$\hat{\mathbf{d}}=\sum_{p=0}^P w_k(\mathbf{S}^H\mathbf{S})^p\mathbf{r}=\left(\left(\left(w_p\mathbf{S}^H\mathbf{S}+\dots\right)\mathbf{S}^H\mathbf{S}+w_1\mathbf{I}\right)\mathbf{S}^H\mathbf{S}+w_0\mathbf{I}\right)\mathbf{r} \quad (19)$$

where multiplication with $\mathbf{S}^H\mathbf{S}$ can be easily realized by resampling with subsequent matched filtering. The (asymptotically) optimum weights w_p can be calculated using results from the theory of large random matrices [24]. Even though these more elaborate methods may yield better bit error rates than the plain Jacobi or Gauss-Seidel algorithm, respectively, the latter are of special importance due to their intuitive interpretation as interference cancellation that allows a simple coupling with nonlinear components as demonstrated in the following section.

IV.5. Nonlinear Interference Cancellation

Linear MUD does not exploit knowledge of the transmit alphabet as the solution region is the entire \square^U (or \square^U in case of BPSK modulation) while the actual transmit vectors are constrained to lie in some discrete signal space. We will restrict our attention to BPSK, so that $\mathbf{d}\in\{-1,1\}^U$. Considering interference cancellation schemes as given in (17) and (18) it is clear that the interference caused by an arbitrary user v will be overestimated whenever $|\hat{d}_v^{(p)}|>1$. Thus, it is advisable to apply some nonlinear function that maps the soft data estimates to the interval $[-1,1]$ after being updated. In [25], simple clipping is proposed which corresponds to the slightly more general mapping

$$\hat{d}_u^{(p+1)}\rightarrow\begin{cases} \hat{d}_u^{(p+1)} & ,|\hat{d}_u^{(p+1)}|<\mathbf{a} \\ \text{sgn}(\hat{d}_u^{(p+1)}) & ,|\hat{d}_u^{(p+1)}|\geq\mathbf{a} \end{cases} \quad (20)$$

for $\mathbf{a} = 1$. However, choosing $\mathbf{a} < 1$ usually leads to faster convergence speed because in this case data estimates are assumed to be reliable enough if $|\hat{d}_u^{(k+1)}|$ exceeds \mathbf{a} and interference caused by the corresponding user is removed completely.

Figure 8 shows the obtained simulation results for our reference system and $\mathbf{a} = 0.4$. After only three iterations, the single-user performance is reached even for a fully loaded system ($J = N_s$), i.e. interference is totally cancelled out. Considering the discrete signal alphabet significantly improves interference cancellation and the MMSE detector is clearly outperformed.

In order to reduce the risk of error propagation, interference cancellation should be combined with channel coding. Regarding the transmitted symbols d_u as encoded bits, soft-input-soft-output decoding algorithms can be employed to obtain estimates $\hat{d}_u^{(p)}$ that include reliability information based on the observation of the whole encoded frame in contrast to uncoded data transmission where consecutive symbols are independent of each other. Although this strategy is very promising in terms of bit error performance, it should be noted that performing soft-output channel decoding during each iteration of the interference cancellation algorithm involves a large computational effort. Apart from that, forward error correction is known to further increase the number of bit errors for very low SINR's. Thus, the previously described linear and nonlinear techniques can be applied to enhance the SINR before starting the interference cancellation loop including channel decoding.

The high potential of the latter approaches is illuminated by Figure 9, where different interference cancellation strategies including channel decoding are compared. It has to be mentioned that the system load is $\mathbf{b} = 2$ and $U = 2N_s$ holds. Therefore, spectral efficiency is twice as high as for conventional TDMA or FDMA systems. Pure PIC with channel decoding does not converge under these severe interference conditions. However, Gauss-Seidel iterations with decoding asymptotically reaches the single-user performance. Convergence can be improved by increasing the SINR at the decoder inputs by a linear MMSE filter [13,14]. In this case, even the PIC reaches the single-user bound. The fastest convergence is achieved by combining linear MMSE and Gauss-Seidel with channel decoding.

V. Conclusions

It has been shown that CDMA systems suffer from severe multi-user interference. Although strong error control coding is able to ensure reliable transmissions for medium system loads, it is

beneficial to apply multi-user detection especially for high system loads. Based on the uplink of an OFDM-CDMA environment, the performances of various multi-user detectors have been demonstrated. Concerning linear approaches, the MMSE detector can be efficiently approximated by iterative strategies like the Gauss-Seidel algorithm to avoid an explicit inversion of the correlation matrix and save computational cost. Taking into account the discrete nature of the signal alphabet, nonlinear elements like clipping or channel decoding have to be incorporated into the iterations. This concept improves performance significantly. Even in the case of an overloaded system, e.g. $U = 2N_s$, the single-user performance can be reached leading to high spectral efficiencies.

References

- [1] Mouly, M., Pautet, M.B., *The GSM-System for mobile Communications*, 1992
- [2] Dahlman, E., Gudmundson, B., Nilsson, M., Sköld, J., UMTS/IMT-2000 Based on Wideband CDMA, *IEEE Communications Magazine*, pages 70-80, September 1998
- [3] Ojanperä, T., Prasad, R., An Overview of Air Interface Multiple Access for IMT-2000/UMTS, *IEEE Communications Magazine*, pages 82-95, September 1998
- [4] Toskala, A., Castro, J., Dahlman, E., Latva-Aho, M., Ojanperä, T., Frames FMA2 Wideband-CDMA for UMTS, *European Transactions on Communications*, vol. 9, no. 4, pages 325-335, August 1998
- [5] Yee, N., Linnartz, J.-P., Fettweis, G., Multi-Carrier CDMA in Indoor Wireless Radio Networks, *IEEE Int. Symp. On Personal, Indoor and Mobile Radio Communications (PIMRC)*, pages D1.3.1-D1.3.5, September 1993
- [6] Fazel, K., Papke, L., On the performance of convolutionally-coded CDMA/OFDM for mobile radio communications systems, *IEEE Int. Symp. On Personal, Indoor and Mobile Radio Communications (PIMRC)*, pages D3.2.1-D3.2.5, September 1993
- [7] Kaiser, S., *Multi-Carrier CDMA Mobile Radio Systems - Analysis and Optimization of Detection, Decoding and Channel Estimation*, VDI-Verlag, German Aerospace Center, 1998

- [8] Dekorsy, A., *Kanalcodierungskonzepte für Mehrträger-Codemultiplex in Mobilfunkssystemen*, University of Bremen, Shaker-Verlag, 2000
- [9] Kühn, V., Dekorsy, A., Kammeyer, K.D., Low Rate Channel Coding for CDMA Systems, *International Journal of Electronics and Communications AEÜ*, vol. 54, no. 6, pages 353-363, 2000
- [10] Verdu, S., *Multiuser Detection*, Cambridge University Press, New York, 1998
- [11] Honig, M., Tsatsanis, M.K., Multiuser CDMA Receivers, *IEEE Signal Processing Magazine*, pages 49-61, May 2000
- [12] Verdu, S., Shamai, S., Spectral Efficiency of CDMA with Random Spreading, *IEEE Transactions on Information Theory*, vol. 45, no. 2, pages 622-640, March 1999
- [13] Kühn, V., Combined MMSE-PIC in Coded OFDM-CDMA Systems, *IEEE Global Conference on Telecommunications (Globecom)*, San Antonio, USA, 2001
- [14] Kühn, V., Linear and Nonlinear Multi-User Detection in Coded OFDM-CDMA Systems, *International Conference on Telecommunications (ICT)*, Bucharest, Romania, 2001
- [15] Frenger, P., Orten, P., Ottosson, T., Code-Spread CDMA using Maximum Free Distance Low-Rate Convolutional Codes, *In Proc. IEEE Int. Symp. on Spread Spectrum Techniques and Applications (ISSSTA)*, Sun City, South Africa, pages 374-378, September 1998
- [16] Benedetto, S., Divsalar, D., Montorsi, G., Pollara, F., Serial Concatenation of Interleaved Codes: Performance Analysis, Design, and Iterative Decoding, *IEEE Transactions on Information Theory*, vol. 44, no. 3, pages 909-926, August 1996
- [17] Frenger, P., Orten, P., Ottosson, T., A. Svensson, *Multi-rate Convolutional Codes*, Technical Report No. 21, 1998, Göteborg
- [18] Honig, M., Madhow, U., Verdu, S., Blinde Adaptive Multiuser Detection, *IEEE Transactions on Information Theory*, vol. 41, no. 4, pages 944-960, July 1995

- [19] Ulukus, S., Yates, R., Optimum Multiuser Detection is Tractable for Synchronous CDMA Systems Using M-Sequences, *IEEE Communications Letters*, vol. 2, no. 4, pages 89-91, April 1998
- [20] Tse, D., Hanly, S., Linear Multiuser Receivers: Effective Interference, Effective Bandwidth and User Capacity, *IEEE Transactions on Information Theory*, vol.45, no. 2, pages 641-657, March 1999
- [21] Golub, G., van Loan, C., *Matrix Computations*, Johns Hopkins University Press, London, 1989
- [22] Moshavi, S., *Multistage Linear Detectors for DS-CDMA Communications*, Ph.D. thesis, University of New York, 1996
- [23] Grant, A., Schlegel, C., Iterative Implementations for Linear Multiuser Detectors, *IEEE Transactions on Communications*, vol. 49, no. 10, pages 1824-1834, October 2001.
- [24] Müller, R., Verdú, S., Design and Analysis of Low-Complexity Interference Mitigation on Vector Channels, *IEEE Journal on Selected Areas in Communications*, vol. 19, no. 8, pages 1429-1441, August 2001
- [25] Yener, A., Yates, R., Ulukus, S., CDMA Multiuser Detection: A Nonlinear Programming Approach, *IEEE Transactions on Communications*, accepted for publication

Figures

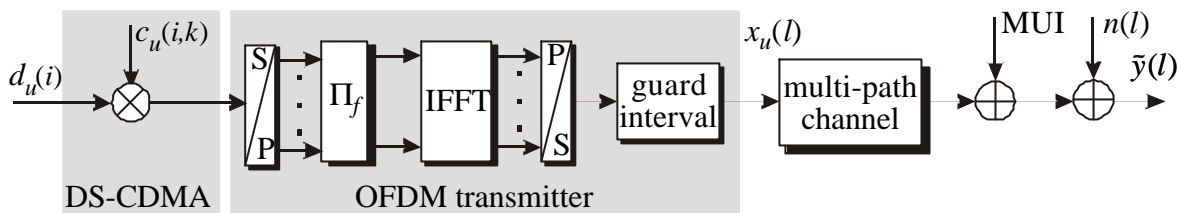


Figure 1: Uplink of a coded OFDM-CDMA system

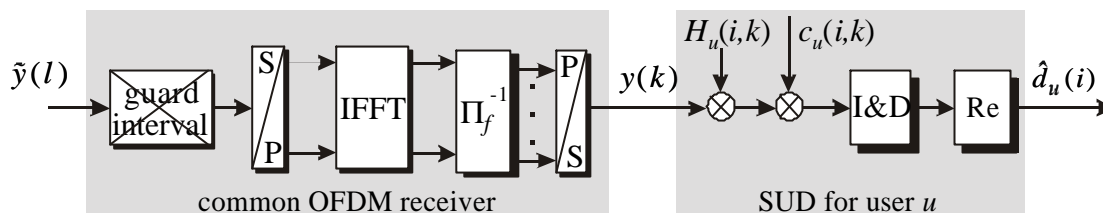


Figure 2: Structure of OFDM-CDMA receiver consisting of common OFDM part and individual single-user detection

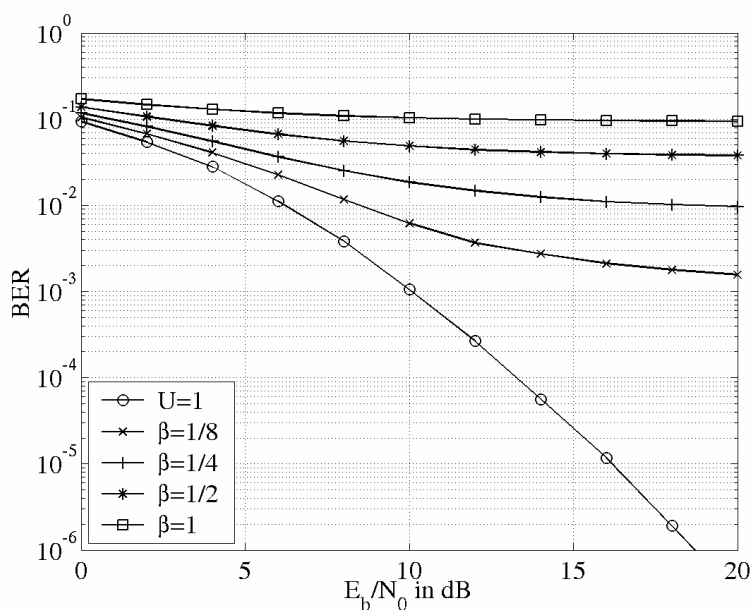


Figure 3: Bit error rate performance of an uncoded OFDM-CDMA system employing single-user detection for different loads $\beta = U / N_s$

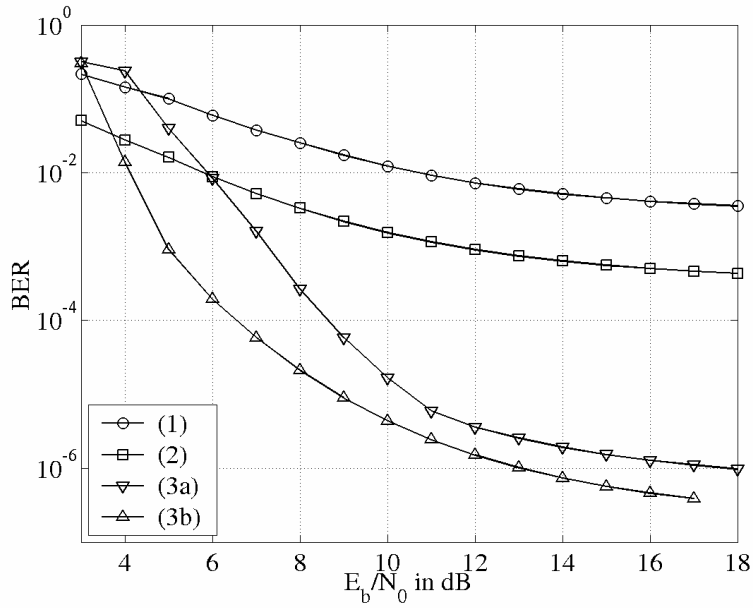


Figure 4: Bit error rate performance of different coding schemes in an OFDM-CDMA system, for a 4-path Rayleigh fading channel and $\beta = 1$,

(1) convolutional code with $L_c=7$ and $R_c=1/2$, $N_s=32$

(2) code-spread system with $L_c=7$ and $R_c=1/64$ according to [17], $N_s=1$

(3) serial concatenation of outer convolutional code ($L_c=3$, $R_c=1/2$) and inner Walsh code

($M=64$), $N_s=3$, a) interleaver of length 600, b) interleaver of length 6000

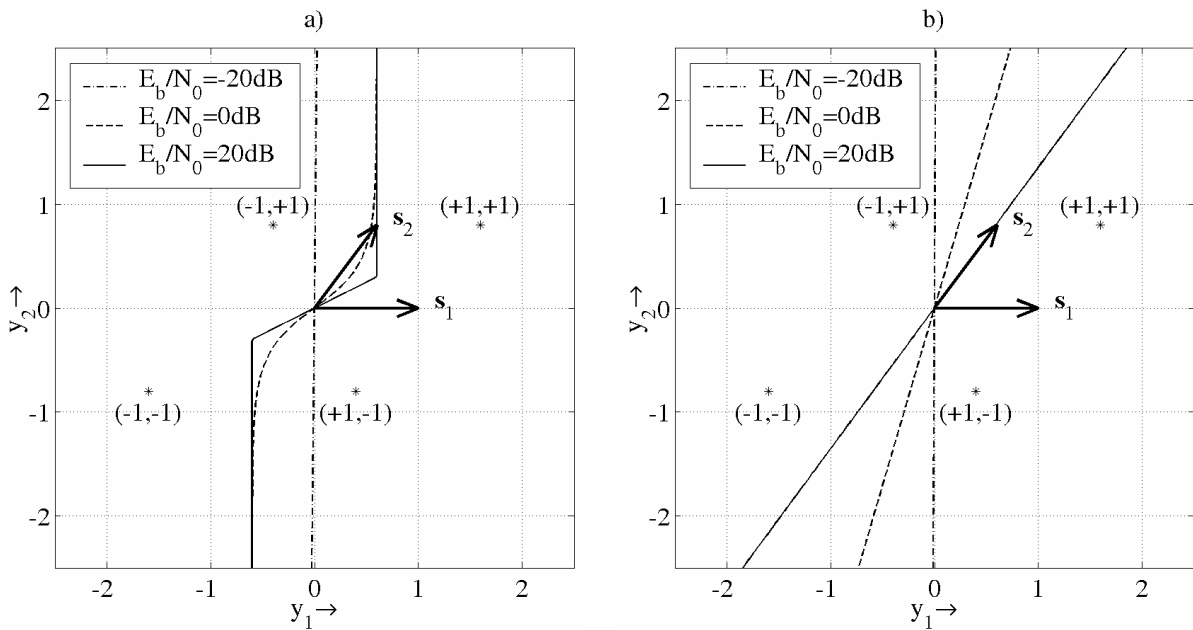


Figure 5: Optimal MAP (a) and linear MMSE (b) decision borders for user 1 in a two-user system with signatures $\mathbf{s}_1 = [1,0]^T$, $\mathbf{s}_2 = [0.6,0.8]^T$ and varying E_b / N_0 . Asterisks denote the noiseless receive signals

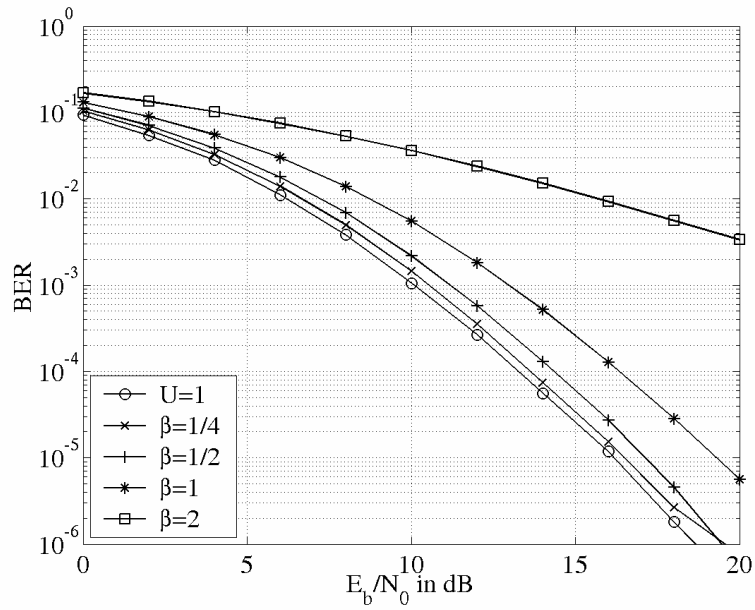


Figure 6: Bit error rate performance of an uncoded OFDM-CDMA system with linear MMSE detection according to (14) for different loads $\beta = U / N_s$

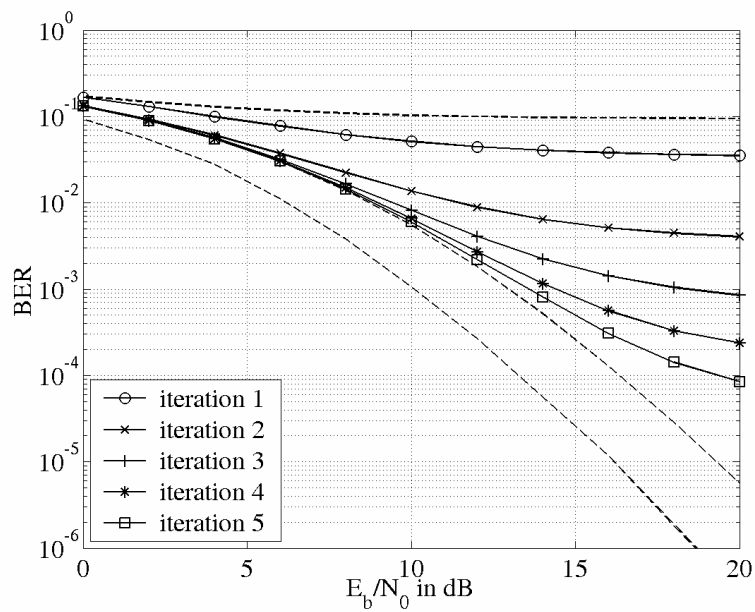


Figure 7: Bit error rate performance of a fully loaded uncoded OFDM-CDMA system with Gauss-Seidel approximation of the MMSE detector. The dashed lines correspond to (from top to bottom) matched filtering, MMSE detection and the single-user bound

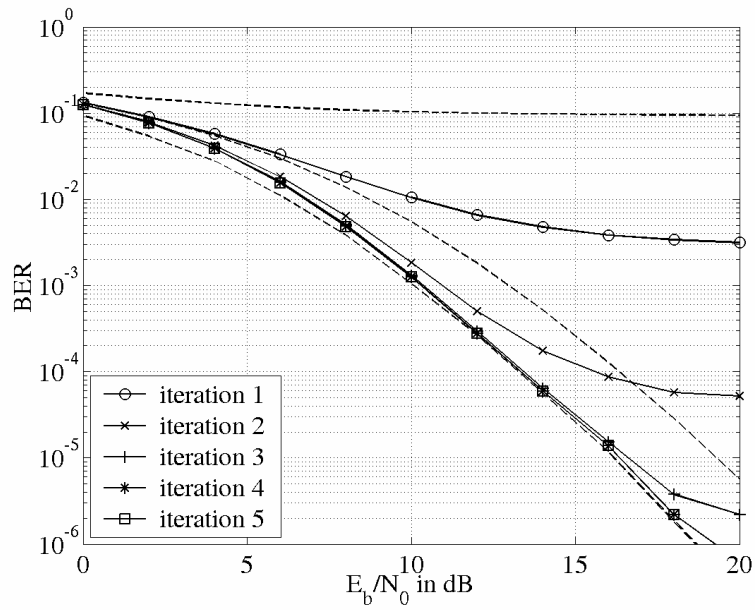


Figure 8: Bit error rate performance of a fully loaded uncoded OFDM-CDMA system with nonlinear interference cancellation ($\alpha = 0.4$). The dashed lines correspond to (from top to bottom) matched filtering, MMSE-detection and the single-user bound

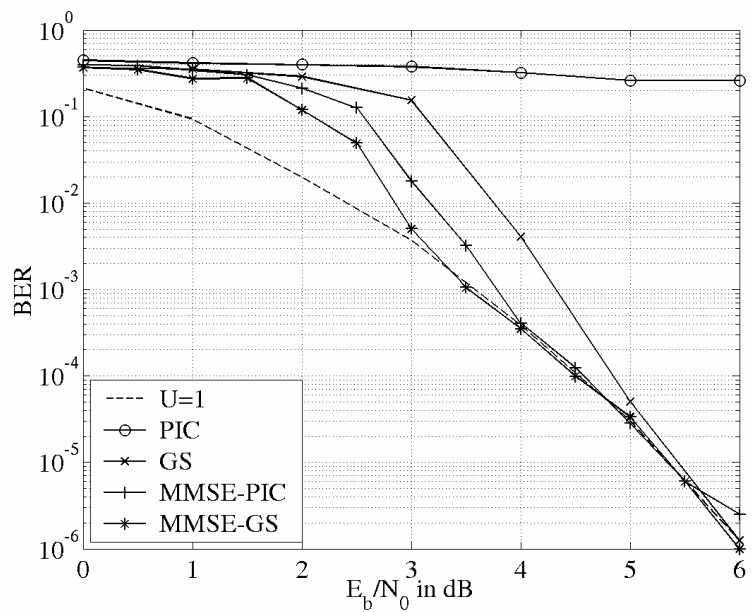


Figure 9: Comparison of parallel and Gauss-Seidel interference cancellation including channel coding with and without linear prefiltering. Results are shown for a doubly overloaded OFDM-CDMA system after 3 iterations